ARCHIVES OF ACOUSTICS
17, 1, 177–189 (1992)

STRUCTURAL AND VISCOELASTIC RELAXATION IN GLYCEROL SOLUTIONS OF ALCALI-METAL WALIDES

M. WACIŃSKI

Institute of Chemistry Silesian University
(40-005 Katowice, ul. Szkolna 9)

R. PŁOWIEC

Institute of Fundamental Technological Research
Polish Academy of Sciences
(00-049 Warszawa, ul. Świętokrzyska 21)

This paper presents the results of density, static viscosity and mechanical impedance measurements of glycerol solutions of electrolytes: LiBr, KBr, NaBr, KCl, RbCl, SeCl, NaF, LiF. The following quantities were calculated: limiting shear moduli, relaxation times, viscous flow activation energy and distribution parameters of viscoelastic relaxation times. Distribution parameters of viscoelastic relaxation times were determined on the basis of the Maxwell's model and the B-E-L model supercooled liquids. The occurrence of a wide spectrum of relaxation times was explained on the basis of the McDuffie's and Litovitz's cluster model and the mechanism proposed by Miles and Hammamoto. On the grounds of the achieved parameters of the relaxation time distribution width it was proved that long-range interactions (structural solvation) caused by the influence of the solvated anion decisively influence structural processes in the analysed solutions.

1. Introduction

Rheologic investigations are of great importance to the cognizance of the structure of liquids and nature of intermolecular forces. Measuring methods based on simple shearing i.e. independent density and temperature changes were applied in these investigations.

Structural rearrangements in liquids due to external shearing forces are of cooperative chamber according to the McDuffie and LITOVIZ [1, 2], because they include the entire group of molecules influenced by the short-range molecular order. Rearrangements are relaxation processes related with the structural relaxation time. The

cooperativity of such rearrangements is reflected in the viscosity of non-Arrhenius liquids which viscosity is not proportional to exp $(-E/RT)$, where E is the activation energy of a viscous flow. The inconformily of the temperature dependence to Eyring's theory can be explained by the fact that it neglects the participation of other molecules in the viscous flow processes and includes only position changes between the molecule and free space neighbouring and the probability of achieving the energy necessary to surmount the potential barrier related with the transition of a single molecule.

The effect of a wide spectrum of dielectric relaxation times in associated liquids was explained on the basis of the described above cluster model if the orientation of a molecule with a permanent dipole moment depends neighbouring molecules, dipole polarization will decays in a nonexponential manner, what can be interpreted as the distribution of characteristic times. Thus, the width of the spectrum should depend on the cluster size; a cooperative process of dislocation and then reconstruction of the molecular order takes place within the cluster.

The cluster model was used to interpret the relaxation of mechanical stresses, i.e. it was accepted that the distribution of structural and viscoelastic relaxation times in caused by the cooperative character of structural changes occurring during volume and shear strains.

The mechanism proposed by MILES and HAMMAMOTO [3] is another mechanism which can be applied to explain the occurrence of a wide spectrum of viscoelastic relaxation time. The occurrence of a wide spectrum is a result of a lack of long-range order in the liquid and of the mutual occurrence of ordered regions with various sizes.

2. Ultrasonic relaxation in glycerol solutions of electrolytes

Previous measurements, performed in multi-hydroxide-alcohol electrolyte solutions have proved that ultrasonic relaxation maintains the same structural character as in pure solvents. All characteristic features of structural relaxation were determined from measurements [4, 5]:

a) within the relaxation region a considerable dispersion of the acoustic wave propagation velocity specific for structural processes was observed.

b) outside the relaxation region ($\omega\tau << 1$) – the relaxation of the absorption coefficient (α) and its classical value (α_{kl}) does not exceed 3, while it can achieve values of several thousands in the case of thermal relaxation.

c) in the non-dispersive region α has a negative temperature coefficient-characteristic of structural processes, while the α/α_{kl} ratio can be accepted as independent of temperature. On the basis of equation

$$\frac{\alpha}{\alpha_{kl}} = 1 + \frac{3}{4}\frac{\eta_v}{\eta_s} \tag{1}$$

where η_v – volume viscosity, η_s – shear viscosity.

We can state that both viscositics are characterized by a more or less identical tempera-

ture dependence (similar activation energy for volume and shear strain). This means that they have similar molecular mechanisms i.e. with an identical structural character of observed relaxation.

d) at law temperatures the absorption coefficient-classical absorption ratio does not exceed 1 what indicates relaxation of the shear viscosity.

Shear impedance measurements in glycerol solutions of electrolytes have confirmed the occurrence of viscoelastic relaxation in the same frequency range in which structural relaxation takes place. Also a shift of the relaxation range towards higher temperatures than in pure glycerol was observed.

3. Viscoelastic relaxation

The interpretation of shear impedance measurements reaction of the investigated solutions to shearing vibrations was based on the relaxation theory as it was done previously in papers [6, 7].

A model created by summing Maxwell elements was used to describe the achieved results. This way the relaxation curve could be described with a continuous spectrum of relaxation times. According to the Maxwell's model the real and imaginary parts of the shear modulus (G' and G'') can be presented of the in a reduced form. Shear impedance components (R_l and x_l) can be presented similarly

$$\frac{G'}{G_\infty} = \int_0^\infty \frac{g_{(x)}\omega^2\tau_{s,0}^2x^2}{1+\omega^2\tau_{s,0}^2x^2}\,dx \tag{2}$$

$$\frac{G''}{G_\infty} = \int_0^\infty \frac{g_{(x)}\omega\tau_{s,0}x}{1+\omega^2\tau_{s,0}^2x^2}\,dx \tag{3}$$

where: $g_{(x)}$ – distribution of relaxation times τ_s standarized with respect to an arbitrary intermediate value $\tau_{s,0}$, $x = \tau_s/\tau_{s,0}$

$$\frac{R_L}{(\rho G_\infty)^{\frac{1}{2}}} = \left\{\frac{\omega^2\tau_{s,0}^2}{2}\int_0^\infty \frac{g_{(x)}x^2}{1+\omega^2\tau_{s,0}^2x^2}\,dx\left\{1+\left[1+\left(\frac{\int_0^\infty \frac{g_{(x)}x}{1+\omega^2\tau_{s,0}^2x^2}\,dx}{\omega\tau_{s,0}\int_0^\infty \frac{g_{(x)}x^2}{1+\omega^2\tau_{s,0}^2x^2}\,dx}\right)^2\right]^{\frac{1}{2}}\right\}^{\frac{1}{2}}\right\} \tag{4}$$

$$\frac{X_L}{(\rho G_\infty)^{\frac{1}{2}}} = \left\{\frac{\omega^2\tau_{s,0}^2}{2}\int_0^\infty \frac{g_{(x)}x^2}{1+\omega^2\tau_{s,0}^2x^2}\,dx\left\{1+\left[\left(\frac{\int_0^\infty \frac{g_{(x)}x}{1+\omega^2\tau_{s,0}^2x^2}\,dx}{\omega\tau_{s,0}\int_0^\infty \frac{g_{(x)}x^2}{1+\omega^2\tau_{s,0}^2x^2}\,dx}\right)^2-1\right]^{\frac{1}{2}}\right\}^{\frac{1}{2}}\right\} \tag{5}$$

In order to calculate the relaxation curve from these equations, distribution functions of relaxation times must be chosen. The Gaussian distribution function was chosen on the basis of LITOVITZ'S and PICCIRELLI'S paper [8]

$$g(\frac{\tau_s}{\tau_s'}) = \frac{b}{\pi^{1/2}} \cdot \frac{\tau_s'}{\tau_s} \exp -[b \ln \frac{\tau_s}{\tau_s'}], \quad 0 < \tau_s < \infty \tag{6}$$

It has maximum for $\tau_s = \tau_s'$. Relaxation curves can be calculated from equations (4) and (5) by substituting τ_s' with $\tau_{s,0}$. The parameter b, which defines the width of the distribution, was determined by comparing resistance curves, calculated from equation (4), with experimental resistance values standarized with respect to the resistance of a solid for investigated liquid $Z = (\rho G_\infty)^{\frac{1}{2}}$ and plotted beginning from frequencies standarized with respect to the Maxwell relaxation time $\omega \eta_s / G_\infty$, where ω – circular frequency $(2\pi f)$, η_s / G_∞ – Maxwell relaxation time. In order to match the relaxation time calculated from equation (4) with experimental points, the theoretical coefficient $\exp(-1/4b^2)$, relating the main time of the Gaussian distribution $\tau_{s,0}$ with the Maxwell relaxation time $\bar{\tau}_s = \frac{\eta_s}{G_\infty}$, i.e. $\tau_{s,0} = \frac{\eta_s}{G_\infty} \exp(1 - \frac{1}{4b^2})$, has to be substitutied by an experimental coefficient a, i.e. $\tau_{s,0} = \frac{\eta_s}{G_\infty} \cdot a$. Discrepancies in relaxation times were stated for many associated liquids. Authors of papers [8, 9] have attributed them to unsatisfactory accuracy of G_∞ determination and to the approximate character of the Gaussian distribution.

In order to become independent of such distribution function of relaxation times and to achieve a better description of viscoelastic relaxation, the precoded liquid model according to A.J. BARLOW, A. ERGINSAV and J. LAMBA [10] was applied. This [B–E–L] model is a combination of mechanical impedance of a Newtonian fluid (Z_N) and a perfectly elastic solid body (Z_s)

$$Z_N = R_N + iX_N = (1 + i)(\pi f \rho \eta_s)^{\frac{1}{2}}, \tag{7}$$

$$Z_s = R_s = (\rho G_\infty)^{\frac{1}{2}} \tag{8}$$

$$\frac{1}{Z_l} = \frac{1}{Z_N} + \frac{1}{Z_s}. \tag{9}$$

Thus we obtain the expression for the complex shear compliance:

$$J^* = J_\infty [\, 1 + \frac{1}{i\omega \tau_s} + \frac{2}{(i\omega \tau_s)^{1/2}} \,] \tag{10}$$

where τ_s is the Maxwell relaxation time $\tau_s = \frac{\eta}{G_\infty}$ and $J_\infty = \frac{1}{G_\infty}$, what satisfactorily describes the behaviour of simple liquids.

The model described above has to be modified in order to use it to describe vis-

coelastic relaxation in complex molecular liquids. This is done by introducing one additional parameter K or two adjustable parameters K and β. When $K = 1$ and $\beta = 0.5$, then the real and imaginary parts of mechanical shear compliance are reduced to the original B-E-L model (equation (10)) and to the Maxwell model with a single relaxation time $K = 0$ ($J' = 1/G_\infty$ and $J'' = 1/(\omega\eta_s)$). The values of parameters K and β were determined with the application of a computer programme, which matches the reduced values of mechanical shear impedance to experimental points:

$$\frac{R_l}{(\rho G_\infty)^{1/2}} = \mathrm{Re}\left[1 + \frac{1}{i\omega\tau_s} + \frac{2K}{(i\omega\tau_s)^\beta}\right]^{-1/2} \tag{11}$$

Calculated values are presented in Tables 5 and 6 and in diagrams.

4. Results of measurements

The following quantities were measured: density, static viscosity, mechanical shear impedance. Methods and apparatus were described in earlier papers [4, 5, 7] and presented at the Winter Schools on Molecular and Quantum Acoustics (1990). Limiting shear modules, relaxation times, activation energy of a viscous flow and distribution parameters of viscoelastic relaxation times were calculated.

Results of density and viscosity measurements are presented in Table 1. Measurements were performed within the temperature range 263–323 K with an accuracy of ± 0.05 K. For lower temperatures density was extrapolated from equation $\rho = A - BT$ and viscosity was calculated from equation $\lg\eta_s = C + DT^{-3}$, where A, B, C and D are constant parameters and T denotes temperature. Achieved density and viscosity values are higher in tested solutions than in pure glycerol. Temperature coefficients standing next to T for density measurements have very similar values. The density in serieses of chlorides and bromides (taking similar concentrations into account) increases in a linear manner in the following sequence: glycerol < KCl < RbCl < CsCl and glycerol < KBr < NaBr < LiBr.

In spite of similar temperature coefficients accompanying T^{-3}, analogic changes of temperature dependence of static viscosities occur in the bromide series only. Such viscosity changes are reflected by activation energies of the viscous flow, which are collected in Table 2. Solutions with similar concentrations are presented in the Table.

Table 3 presents values of the limiting shear modulus G_∞, which is considered to be a characteristic quantity describing the liquids molecular structure. Achieved results indicate a minimum influence of electrolytes on the rheological properties of glycerol in the elastic region. The convergence of moduli lies within the measuring error accepted as ± 10%. Static viscosity and limiting shear modulus changes determine changes of the Maxwell relaxation time. Its values are gathered in Table 4.

Mechanical shear impedance measurements were performed in the temperature range 223–303 K and frequency range 0.5–500 MHz. Parameters of the distribution width of viscoelastic relaxation times (b), as well as theoretical and experimental ratio

Table 1

Investigated system		Density (ρ) [$kg \cdot m^{-3}$]		Static viscosity ($\lg \eta_s$) [$N \cdot s \cdot m^{-2}$]	
		A	*B*	*C*	*D*
Glycerol		$1.4360 \cdot 10^3$	$-6.012 \cdot 10^{-1}T$	−3.6344	$+ 9.3908 \cdot 10^{7}R^{-3}$
Glycerol – KCl	(0.6023)	$1.4388 \cdot 10^3$	$-5.184 \cdot 10^{-1}T$	−3.8099	$+ 1.0044 \cdot 10^{8}T^{-3}$
Glycerol – RbCl	(0.5512)	$1.4707 \cdot 10^3$	$-5.955 \cdot 10^{-1}T$	−3.8567	$+ 1.0001 \cdot 10^{8}T^{-3}$
Glycerol – CsCl	(0.3474)	$1.4725 \cdot 10^3$	$-5.937 \cdot 10^{-1}T$	−3.6850	$+ 9.9849 \cdot 10^{7}T^{-3}$
Glycerol – LiBr	$(0.3742 \cdot 10)$	$1.6064 \cdot 10^3$	$-5.917 \cdot 10^{-1}T$	−3.4182	$+ 1.1145 \cdot 10^{8}T^{-3}$
	$(0.1350 \cdot 10)$	$1.4850 \cdot 10^3$	$-5.984 \cdot 10^{-1}T$	−3.6836	$+ 1.0175 \cdot 10^{8}T^{-3}$
	$(0.1199 \cdot 10)$	$1.4773 \cdot 10^3$	$-5.959 \cdot 10^{-1}T$	−3.6908	$+ 1.0125 \cdot 10^{8}T^{-3}$
Glycerol – NaBr	$(0.1191 \cdot 10)$	$1.5860 \cdot 10^3$	$-7.147 \cdot 10^{-1}T$	−3.5426	$+ 1.0354 \cdot 10^{8}T^{-3}$
	(0.5791)	$1.5027 \cdot 10^3$	$-6.349 \cdot 10^{-1}T$	−3.6706	$+ 1.0085 \cdot 10^{8}T^{-3}$
Glycerol – KBr	$(0.1786 \cdot 10)$	$1.5408 \cdot 10^3$	$-5.814 \cdot 10^{-1}T$	−3.7340	$+ 9.6825 \cdot 10^{7}T^{-3}$
	(0.8638)	$1.4893 \cdot 10^3$	$-6.029 \cdot 10^{-1}T$	−3.7097	$+ 9.5124 \cdot 10^{7}T^{-3}$
Glycerol – LiF	(0.2833)	$1.4021 \cdot 10^3$	$-5.723 \cdot 10^{-1}T$	−3.7688	$+ 9.9166 \cdot 10^{7}T^{-3}$
Glycerol – NaF	(0.09864)	$1.4345 \cdot 10^3$	$-5.982 \cdot 10^{-1}T$	−3.7636	$+ 9.4946 \cdot 10^{7}T^{-3}$
Glycerol – $FeCl_3$	(0.06715)	$1.4284 \cdot 10^3$	$-5.460 \cdot 10^{-1}T$	−3.4155	$+ 9{,}2424 \cdot 10^{7}T^{-3}$
	(0.1069)	$1.4404 \cdot 10^3$	$-5.702 \cdot 10^{-1}T$	3.3328	$+ 9.1404 \cdot 10^{7}T^{-3}$
	(0.1693)	$1.4438 \cdot 10^3$	$-5.614 \cdot 10^{-1}T$	−3.2573	$+ 9.1768 \cdot 10^{7}T^{-3}$
	(0.3058	$1.4707 \cdot 10^3$	$-5.919 \cdot 10^{-1}T$	−3.3343	$+ 9.9207 \cdot 10^{7}T^{-3}$
	(0.4015)	$1.4904 \cdot 10^3$	$-6.157 \cdot 10^{-1}T$	−3.6218	$+ 1.1342 \cdot 10^{8}T^{-3}$

Concentration of the dissolved substance, i.e. mole per kg of solvent (glycerol) is given in brackets

of the main time of the Gaussian distribution to the Maxwell time have been calculated on the basis of these measurements. They are presented in Table 5.

In order to make the interpretation of results independent of the accepted relaxation time distribution function and in order to achieve better matching (especially for $FeCl_3$ solutions) of measurements and theoretical relaxation curves, the B-E-L supercooled liquid model was applied. Calculated values of the parameter K (matching with one parameter), as well as K and β (matching with two parameters) are collected in Table 6 and presented in a graphical form.

From the achieved results we can draw a conclusions that glycerol solutions of chlorides and fluorides widen the spectrum of viscoelastic relaxation times with respect

Table 2

Activation energy (E_a)
[$KJ \cdot mol^{-1}$]

Temperature	Glycerol	KCl	RbCl	CsCl	LiBr	NaBr	KBr	LiF	NaF
303—293	60.6	64.7	62.9	63.5	64.6	65.1	61.4	63.7	62.5
293—283	66.9	69.1	69.1	69.2	69.3	69.3	66.9	67.9	67.2
283—273	71.8	74.0	74.8	74.2	76.4	77.4	71.8	74.8	72.8
273—263	77.2	80.4	80.1	79.7	80.8	78.5	77.4	79.1	78.3
263—253	83.4	86.5	86.1	86.5	86.9	86.8	83.5	84.8	84.1
253—243	89.9	90.1	93.5	93.2	96.5	95.9	90.3	95.0	92.9
243—223	199.6	211.2	212.2	212.1	212.6	211.4	205.3	208.1	207.1

Table 3

Limiting shear modulus (G_∞)
[Nm^{-2}] $\cdot 10^9$

Investigated system		Temperature K					
		218	223	228	233	238	243
Glycerol		3.77	3.65	3.52	3.40	3.28	3.16
Glycerol-KCl	(0.6023)	3.73	3.60	3.48	3.38	3.25	3.12
Glycerol-RbCl	(0.5512)	3.74	3.65	3.56	3.47	3.38	3.26
Glycerol-CsCl	(0.3474)	3.76	3.67	3.58	3.49	3.40	3.28
Glycerol-LiBr	(3.742)	3.77	3.65	3.56	3.48	3.39	3.31
	(1.350)	3.76	3.66	3.57	3.48	3.40	3.31
	(1.199)	3.76	3.67	3.58	3.48	3.40	3.29
Glycerol-NaBr	(1.191)	3.79	3.68	3.57	3.47	3.39	3.27
	(0.5791)	3.73	3.60	3.48	3.38	3.25	3.12
Glycerol-KBr	(1.786)	3.74	3.65	3.56	3.48	3.39	3.30
	(0.8638)	3.76	3.67	3.58	3.49	3.40	3.30
Glycerol-LiF	(0.2833)	3.74	3.64	3.57	3.46	3.39	3.29
Glycerol-NaF	(0.09864)	3.75	3.66	3.57	3.48	3.39	3.29

Table 4

Maxwell's relaxation time (τ_s) [s]

Investigated system		Temperature K 223.15	243.15	274.15	293.15
Glycerol		$1.78 \cdot 10^{-5}$	$2.51 \cdot 10^{-7}$	$3.40 \cdot 10^{-9}$	$5.10 \cdot 10^{-10}$
Glycerol-KCl	(0.6023)	$4.59 \cdot 10^{-5}$	$4.10 \cdot 10^{-7}$	$4.74 \cdot 10^{-9}$	$6.17 \cdot 10^{-10}$
Glycerol-RbCl	(0.5512)	$3.84 \cdot 10^{-5}$	$3.85 \cdot 10^{-7}$	$4.05 \cdot 10^{-9}$	$5.35 \cdot 10^{-10}$
Glycerol-CsCl	(0.3474)	$5.52 \cdot 10^{-5}$	$5.57 \cdot 10^{-7}$	$5.93 \cdot 10^{-9}$	$7.82 \cdot 10^{-10}$
Glycerol-LiBr	(1.120)	$7.13 \cdot 10^{-5}$	$7.09 \cdot 10^{-7}$	$6.91 \cdot 10^{-9}$	$8.76 \cdot 10^{-10}$
Glycerol-NaBr	(0.5791)	$6.88 \cdot 10^{-5}$	$7.03 \cdot 10^{-7}$	$7.09 \cdot 10^{-9}$	$8.55 \cdot 10^{-10}$
Glycerol-KBr	(0.8638)	$2.62 \cdot 10^{-5}$	$3.06 \cdot 10^{-7}$	$3.76 \cdot 10^{-9}$	$5.31 \cdot 10^{-10}$
Glycerol-LiF	(0.2833)	$3.87 \cdot 10^{-5}$	$4.25 \cdot 10^{-7}$	$4.56 \cdot 10^{-9}$	$6.05 \cdot 10^{-10}$
Glycerol-NaF	(0.09864)	$3.57 \cdot 10^{-5}$	$3.95 \cdot 10^{-7}$	$4.16 \cdot 10^{-9}$	$5.65 \cdot 10^{-10}$

Concentrations of dissolved substances in moles per kg of solvent

Table 5

Investigated system		b	$\exp -\frac{1}{4b^2}$	a
Glycerol		0.40	0.21	0.19
Glycerol-LiF	(m = 0.2833)	0.30	0.06	0.14
Glycerol-NaF	(m = 0.09864)	0.38	0.18	0.14
Glycerol-KCl	(m = 0.6023)	0.38	0.18	0.12
Glycerol-RbCl	(m = 0.5512)	0.39	0.19	0.12
Glycerol-CsCl	(m = 0.3474)	0.39	0.19	0.12
Glycerol-$FeCl_3$	(m = 0.06715)	0.33	0.10	0.11
	(m = 0.1069)	0.33	0.10	0.11
	(m = 0.1693)	0.32	0.09	0.11
	(m = 0.3058)	0.30	0.06	0.07
	(m = 0.4015)	0.30	0.06	0.07
Glycerol-LiBr	(m = 1.199)	0.45	0.29	0.18
	(m = 1.350)	0.45	0.29	0.18
	(m = 3.742)	0.50	0.37	0.02
Glycerol-NaBr	(m = 0.5791)	0.45	0.29	0.22
	(m = 1.191)	0.45	0.29	0.21
Glycerol-KBr	(m = 0.8638)	0.42	0.24	0.24
	(m = 1.786)	0.44	0.27	0.26

Table 6

Investigated system		K	matching	K	β	matching
Glycerol		0.95	0.99954	1.00	0.56	0.99991
Glycerol-LiF	(m = 0.2833)	1.87	0.98860	1.98	0.56	0.99732
Glycerol-NaF	(m = 0.09864)	1.38	0.99990	1.46	0.54	0.99972
Glycerol-KCl	(m = 0.6023)	1.38	0.99792	1.46	0.56	0.99942
Glycerol-RbCl	(m = 0.5512)	1.22	0.99935	1.46	0.60	0.99995
Glycerol-CsCl	(m = 0.3474)	1.22	0.99943	1.45	0.58	0.99998,
Glycerol-$FeCl_3$	(m = 0.06715)	1.38	0.99946	1.28	0.44	0.99996
	(m = 0.1069)	1.31	0.99383	1.20	0.42	0.99876
	(m = 0.1693)	1.47	0.99870	1.34	0.44	0.99956
	(m = 0.3058)	1.70	0.99699	1.58	0.44	0.99919
	(m = 0.4015)	1.87	0.99094	1.56	0.40	0.99870
Glycerol-LiBr	(m = 1.199)	0.74	0.99990	0.88	0.45	0.99999
	(m = 1.350)	0.72	0.99906	0.88	0.46	0.99993,
Glycerol-LiBr	(m = 3.742)	0.52	0.99934	0.54	0.48	0.99990
Glycerol-NaBr	(m = 0.5791)	0.84	0.99895	0.88	0.60	0.99996
	(m = 1.191)	0.92	0.99762	0.98	0.60	0.99992
Glycerol-KBr	(m = 0.8638)	0.83	0.99861	0.88	0.48	0.99985
	(m = 1.786)	0.85	0.99962	0.90	0.56	0.99996

Values of parameter K determined with accuracy of 0.01

to the solvent-glycerol. For LiF b = 0.30, for NaF, KCl, RbCl, CsCl parameter b = 0.39, while for $FeCl_3$ solutions the parameter of distribution width is contained within the range 0.30–0.33.

An opposite effect is observed for bromide solutions. They limit the relaxation time spectrum in comparison to pure glycerol which has parameter b equal to 0.40. For LiBr and NaBr solutions b = 0.45 (excluding the concentrated LiBr solution, where b achieves a value of 0.50). As for KBr solutions parameter b is equal to 0.42.

In accordance with the cluster interpretation of the relaxation time distribution, the cooperativity of structural processes is of greater importance in chloride and fluoride solutions than in pure glycerol, while in bromide solutions it is of less importance. Cooperativity causes a non-exponential stress decay what is expressed by a wide distribution the of time spectra. Hence we can infer that cooperativity increase results in an increase of the width of the relaxation time distribution. On the other hand applying the

model proposed by Miles and Hammamoto we can conclude that the increase of the spectrum width with respect to the spectrum for glycerol suggests that clusters for chlorides and fluorides are more developed, and for bromide solutions there is an opposite effect.

Research concerning the dissolution entropy of water solutions of electrolytes [11] indicated that changes in water structure exceed the first coordination sphere. Values achieved for electrolytes differ from the obtained from value the effect of particle freezing and the ordering effect of the ions electric field. This difference will be characteristic of the structural contribution of individual ions. For halide anions (except F^-) negative values were obtained:

$$S = F^- (+ 3.5), Cl^- (- 10.2), Br^- (- 13.9), J^- (- 17.9).$$

These values may indicate that the closest layer of water molecules freezes, while the large radius and electric field of the ion cause such a change in the orientation of water particles that they are less ordered in the second layer than in pure water. The introduction of an ion gives rise to two competitive effects: formation of intramolecular hydrogen bands or ion-dipole interaction, and the effect of water structure distruction. The destructive action of an ion increases when the ion's radius increases. According to Pauling radii of ions are equal to values given in A:

cations - Li^+ (0.60), Na^+ (0.95), K^+ (1.33), Rb^+ (1.48), Cs^+ 1.69),

anions - F^- (1.36), Cl^- (1.81), Br^- (1.95), J^- (2.16).

The F^- ion with a radius and polarizability only slightly differing from the respective values of oxygen in water can cause the ordering of particles resembling the order in water.

SAMOJŁOW [12] reached a similar conclusion on the basis of considerations concerning ion hydratation. He defines hydratation as the reaction of an ion to the translational motion of water molecules. The time a H_2O molecule stays (in equilibrium state) near an ion with respect to the time a H_2O molecule stays (in equilibrium state) in pure water in the hydratation measure. If $t_1 > t_0$, then the effect of positive hydratation takes place; while, if $t_1 < t_0$, then negative hydratation occurs. It results from presented calculations that F^- ions correspond to positive hydratation, while K^+, Cl^-, Br^-, J^- correspond to negative hydratation.

It results from our measurements that in glycerol solutions not only F^- ions but also Cl^- ions introduce an order in the solvents structure while larger Br^- anions have a disturbing effect as it happens in aqueous solutions.

Furthermore, a comparison of the obtained results indicates a lack of a distinctive cation effect. The anion has a prevailing influence on the width of the distribution of relaxation times. Parameter b accepts the value of 0.45 for LiBr (except for the highly concentrated solution, $m = 3.742$), NaBr and KBr solutions.

On the basis of the achieved results we can see that structural processes are affected not by direct ion-dipole or ion-induced dipole interaction (i.e. Coulomb solvation), but

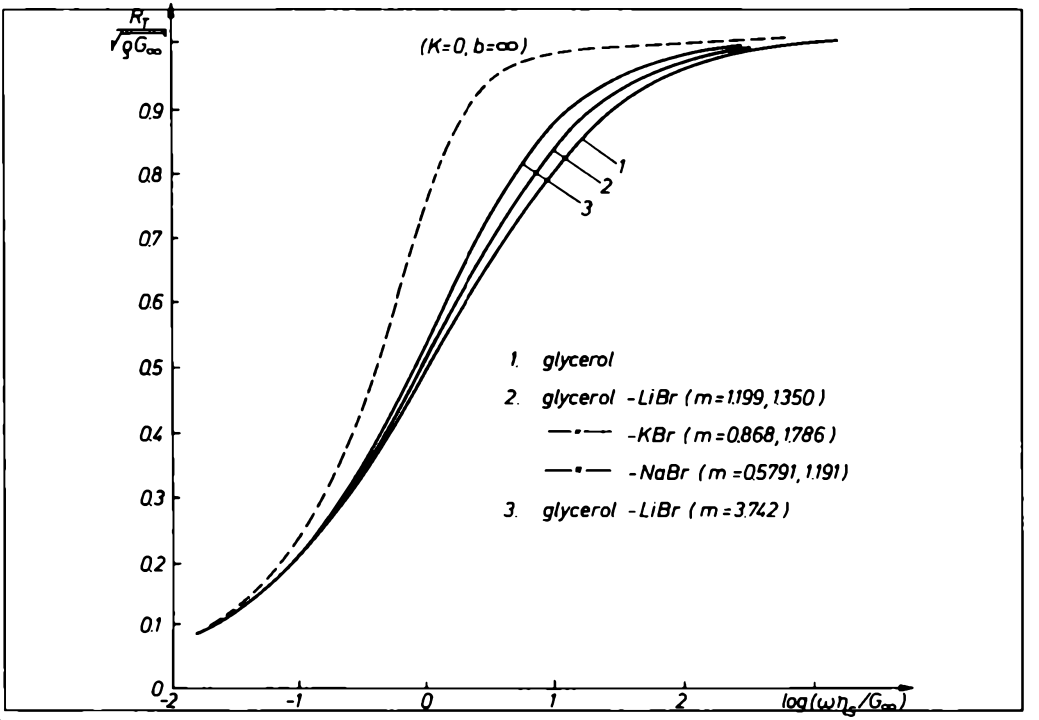
$\frac{R_T}{\sqrt{\rho G_\infty}}$
(K=0, b=∞)
0.9
0.8
0.7
0.6
0.5
0.4
0.3
0.2
0.1
0
-2
-1
0
1
2
log(ωη_S/G_∞)
1
2
3
1. glycerol
2. glycerol - LiBr (m=1.199, 1.350)
—•— -KBr (m=0.868, 1.786)
—•— -NaBr (m=0.5791, 1.191)
3. glycerol - LiBr (m=3.742)

FIG. 1

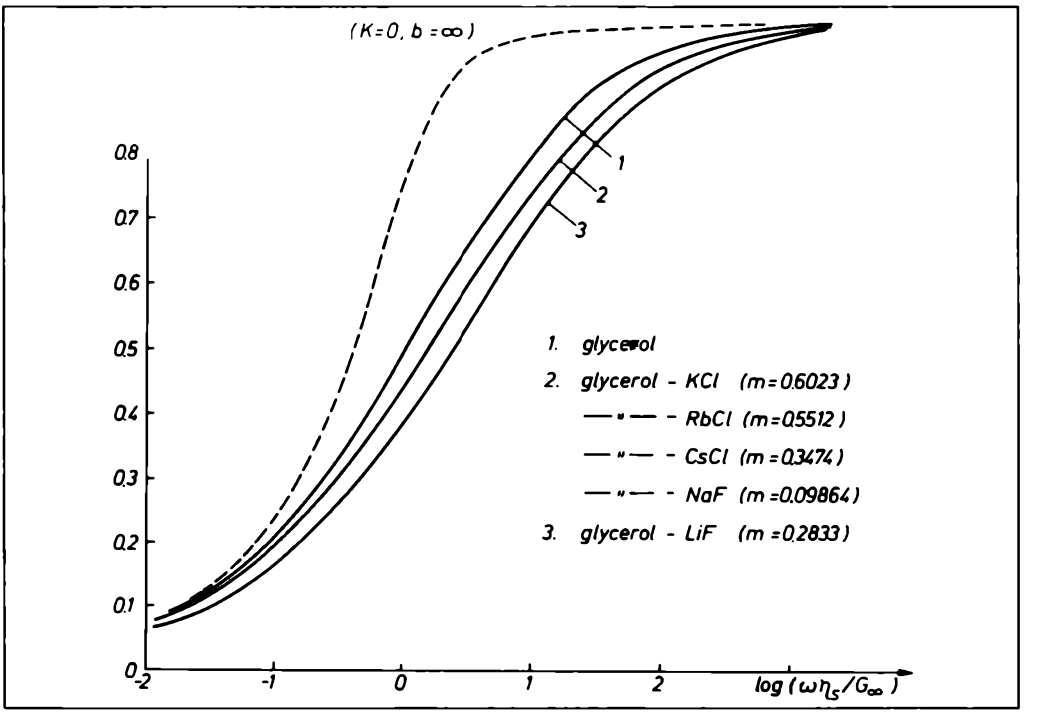
(K=0, b=∞)
0.8
0.7
0.6
0.5
0.4
0.3
0.2
0.1
0
-2
-1
0
1
2
log(ωη_S/G_∞)
1
2
3
1. glycerol
2. glycerol - KCl (m=0.6023)
—•— - RbCl (m=0.5512)
— " — - CsCl (m=0.3474)
— " — - NaF (m=0.09864)
3. glycerol - LiF (m=0.2833)

FIG. 2

also by long-range interactions, i.e. secondary solvation (structural), due to the influence of solvated ion or ion pair.

Calculations carried out by KOŁOS and PIELA [13] indicate the existence of a vibration coupling effect (Raman spectra) in a hydrogen bond between water and proton acceptors. Investigations on changes in band intensities of stretching vibrations in the Raman spectrum of water [14] caused by halide and ions prove that their bonds with water become weaker in the following series: $J^- > Br^- > Cl^- > F^-$. The analysis of frequency and intensity changes of the OH group band leads to a conclusion that the anion has a decisive effect on the parameters of the spectrum. If cations caused hydrogen bands to break and then interacted with free electron pairs in oxygen, this would be reflected in the vibration spectrum of water. Probably, after breaking hydrogen bonds, anions form their own, new bonds with water that determine the changes in the vibration spectrum of water.

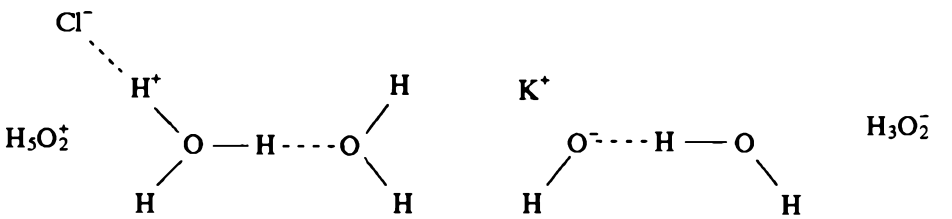

On the basis of the water hydratation model presented by A. JUSZKIEWICZ (XIXth Winter School on Molecular and Quantum Acoustics, Wisła, 1990) we can believe that halide ions are built in pseudocrystalline groups of the solvent. STEWARD'S [14] radiographic examinations led to the same conclusion. He did not state a maximum in obtained diffraction patterns of alcoholic solutions of LiCl, corresponding with free Cl^- ions. Also investigations of water molecule structure in stable hydrates by nuclear magnetic resonance NMR [15] indicated the existence of hydrogen bonds with ions with high electronegativity and hence confirmed JUSZKIEWICZ'S results.

It seems interesting to compare the presented results with earlier measurements in glycerol solutions of $FeCl_3$ [16, 17]. A wide spectrum of viscoelastic relaxation times was obtained for these solutions. It is related to the formation of fairly stable solvation complexes with 3d orbitals of the Fe^{+3} ion. The B-E-L model and the Maxwell model with a symmetric normal distribution function were used to describe the relaxation curve. However the description with the Maxwell model was found to be unsatisfactory because a certain asymmmetry in the distribution of relaxation times occured. Probably equilibrium states between various ferric (III) chloride complexes are responsible for this asymmetry and for the dependence of relaxation times on concentration.

In the case of the investigated electrolytes, such a concentration-dependence was observed for the most concentrated LiBr solution ($m = 3.742$ only). This may lead to a conclusion that a cation effect can take place for ions with great complexing power.

Such a conclusion is confirmed by research performed by KĘCKI [18] on aqueous solutions of chlorides with various cations. It has proved that a similar effect as that caused by large anions is observed in the case of cations with high complexing power, e.g. Cd^{+2}, Zn^{+2}. Whereas for ions which do not form complexes, with high charge density, the effect was much smaller, e.g. Mg^{+2} or Al^{+3}.

5. Conclusions

This paper has confirmed our assumption that the presence of an electrolyte, which changes the molecular order in the solvent, should radically influence relaxation parameters, the value of the relaxation time and its distribution, particularily.

The achieved results indicate the usefulness of rheological studies, based on simple shear especially, not only in technological problems where viscous flow occurs, but also in the recognition of the structure of liquids electrolyte solutions and intermolecular interactions occuring in such solutions.

References

[1] G.E. MCDUFFIE Jr, T.A. LITOVITZ, J. Chem. Phys., **37**, 1699 (1962).
[2] T.A. LITOVITZ, G.E. MC DUFFIE Jr, J. Chem. Phys., **39**, 729 (1963).
[3] D.C. MILES, D.S. HAMMAMOTO, Nature, **193**, 644 (1962).
[4] S. ERNST, J. GLIŃSKI, M. WACIŃSKI, Acustica, **40**, 128 (1978).
[5] S. ERNST, M. WACIŃSKI, Acustica, **47**, 1 (1980).
[6] S. ERNST, M. WACIŃSKI, R. PŁOWIEC, Acustica, **45**, 30 (1980).
[7] S. ERNST, M. WACIŃSKI, Mat. Sci., **III 3**, 75 (1977).
[8] R. PICCIRELLI, T.A. LITOVITZ, J.A.S.A., **29**, 1009 (1957).
[9] R. MEISTER, C.J. MARHOEFFER, R. SCIAMANDA, L. COTTER, T.A. LITOVITZ, J. Appl. Physics, **31**, 854 (1960).
[10] A.J. BARLOW, A. ERGINSAV, J. LAMB, Proc. Roy. Soc., **A 298**, 481 1967.
[11] H.S. FRANK, M.W. EVANS, J. Chem. Phys., **13**, 507 (1945).
[12] O.J. SAMOJLOV, *Struktura vodnych roztvorov elektrolitov i gidratacija jonov*, Izd. Akad. Nauk SSSR Moskva 1957.
[13] W. KOŁOS, L. PIELA, Roczniki Chemii, **40**, 713 (1966).
[14] Z. KĘCKI, Pr. zb. *Spektralne badanie struktury roztworów elektrolitów*, PWN, Warszawa 1969.
[15] J.W. MC GRATH, A.A. SILVADI, J. Chem. Phys., **34**, 322 (1961).
[16] S. ERNST, M. WACIŃSKI, J. GLIŃSKI, R. PŁOWIEC, Acustica, **47**, 292 (1981).
[17] M. WACIŃSKI, R. PŁOWIEC, Arch. Akustyki, **16**, 1, (1981).
[18] Z. KĘCKI, Roczniki Chemii, **38**, 329 (1964).

Received on August 10, 1990